Available online at www.sciencedirect.com
SCIENCE DIRECT®
Journal of Fluorine Chemistry 120 (2003) 99–104
JOURNAL OF FLUORINE CHEMISTRY
www.elsevier.com/locate/jfluchem

Surface properties of fluorinated single-walled carbon nanotubes

Young Seak Lee[a,b,*], Tae Hyun Cho[b], Byoung Ky Lee[c], Jae Seong Rho[c], Kay Hyeok An[d], Young Hee Lee[d]

[a]*Department of Chemical Engineering, Nanotechnology Center, Sunchon National University, Sunchon 540-742, South Korea*
[b]*Department of Chemical Engineering, Clemson University, Clemson, SC 29634, USA*
[c]*Department of Fine Chemical Engineering, Chungnam National University, 305-764 Chungnam, South Korea*
[d]*Department of Physics, Sungkyunkwan University, Suwon 440-746, South Korea*

Received 1 August 2002; received in revised form 11 October 2002; accepted 18 October 2002

Abstract

Single-walled carbon nanotubes (SWCNTs) were fluorinated at several different temperatures. The change of atomic and electronic structures of fluorinated SWCNTs was investigated using X-ray photoelectron spectroscopy (XPS), electrical resistivity measurements and transmission electron microscopy (TEM). The amount of doped fluorine increases with increasing doping temperature, and the fluorine atoms are covalently attached to the side-wall of the SWCNTs. From Raman spectra and HRTEM study, the strong fluorination on the SWCNTs leads to the breaking of carbon–carbon bonds and the disintegration of tube structure. Several intermediate phases of fluorinated SWCNTs are observed during e-beam irradiation in HRTEM.

Keywords: Fluorination; Single walled carbon nanotubes (SWCNTs); X-ray photoelectron spectroscopy (XPS); Surface property; Transmission electron microscopy (TEM)

1. Introduction

Since the discovery of single-wall carbon nanotubes (SWCNTs) [1], the nanometer-scale carbon tubes as a novel form of carbon materials have attracted great interest not only in scientific fields but also in the fields of nanotechnology applications, such as electronic devices and energy related applications. There has been a flurry of research activity aimed for understanding their physical properties [2], and developing novel uses for them [3]. In spite of the intensive researches on carbon nanotubes (CNTs), applications of CNTs to practical use of electronic and energy storage devices are still limited by the number of reasons. Carbon nanotubes are chemically inert and mechanically hard material due to their strong covalent bonds. Functionalization of a CNT wall sometimes leads to serious modification of the atomic structures. Sidewall functionalization may enhance the performance of carbon nanotubes in hydrogen storage, secondary battery, and supercapacitor.

Since fluorination is one of the most effective chemical methods to modify and control physicochemical properties in a wide range, fluorination of new forms of carbon materials are of great interest. Recently there have been several reports on sidewall functionalization of single walled carbon nanotubes (SWCNTs) by fluorination [4,5]. Mickelson et al. reported that fluorinated nanotube are highly resistive and can survive at temperatures up to 325 °C [4]. This subject is of great interest for a wide variety of sidewall chemical functionalizations. Mickelson et al. has also shown in further work that fluorinated SWCNTs (F-SWCNTs) are dissolved well in alcohol solvents to give long-living metastable solution [5]. Consequently, interesting routes to prepare a wide variety of functionalized nanotubes have been developing though the solution chemistry of fluorinated SWCNTs [6]. The fluorination was reported for commercially available multiwall carbon nanotubes (MWCTs) [7].

Although several reviews on fluorinated carbon nanotubes are available [5–9], in this paper more recent topics in this field is covered with an emphasis on the surface property (electronic and structural change) of fluorinated single walled carbon nanotubes. In this study, single-walled carbon nanotubes (SWCNTs) were fluorinated at several different

* Corresponding author. Tel.: +82-61-750-3586; fax: +81-61-750-3580.
E-mail address: leeys@sunchon.ac.kr (Y.S. Lee).

0022-1139/02/$ – see front matter © 2002 Elsevier Science B.V. All rights reserved.
doi:10.1016/S0022-1139(02)00316-0

temperatures. The change of atomic and electronic structures of fluorinated SWCNTs powder as a function of fluorination temperature was investigated using X-ray photoelectron spectroscopy (XPS), electrical resistivity measurements and transmission electron microscopy (TEM).

2. Results and discussion

Fig. 1 shows XPS C 1s curve fit spectra for the fluorinated SWCNTs at various temperatures. The spectra of the undoped SWCNTs (a) give three peaks, that represent sp^2 carbon (peak 1, 284.3 eV), sp^3 carbon (peak 2, 285.0 eV) and oxygen related (carboxyl) group (peak 3, 288.5 eV). After fluorination, the intensity of sp^2 peak becomes broader and significantly reduced with increasing reaction temperatures. This sp^2 peak shape largely changes at high temperatures above 250 °C. A variety of news peak also appear at 287.0 (peak 4, semi-ionic C−F), 288–289 (peak 6, nearly covalent C–F) and 292.0–294.05 (peak 5 and peaks 7–8, covalent CF_2, CF_3), respectively. These peaks at high binding energy side indicate the existence of various carbon species bonded to fluorine. The C 1s peaks observed at 291.2–294.6 eV were ascribed to sp^3 hybridized carbon atoms with covalent C–F bonds, which are similar to those in the covalent compounds, graphite fluorides, $(CF)_n$ and $(C_2F)_n$ [8].

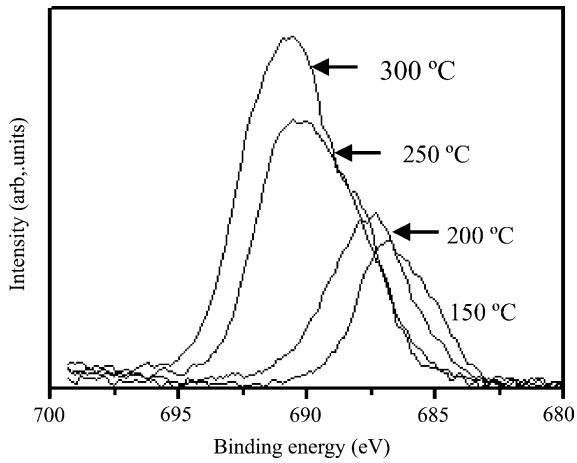

Fig. 2. XPS F 1s spectra of the undoped and fluorinated SWCNTs at various fluorination temperatures.

Fig. 2 shows XPS F 1s spectra of F-SWCNTs at various reaction temperatures. As shown in this figure, in contrast with the C 1s spectra, the F 1s spectra showed symmetric

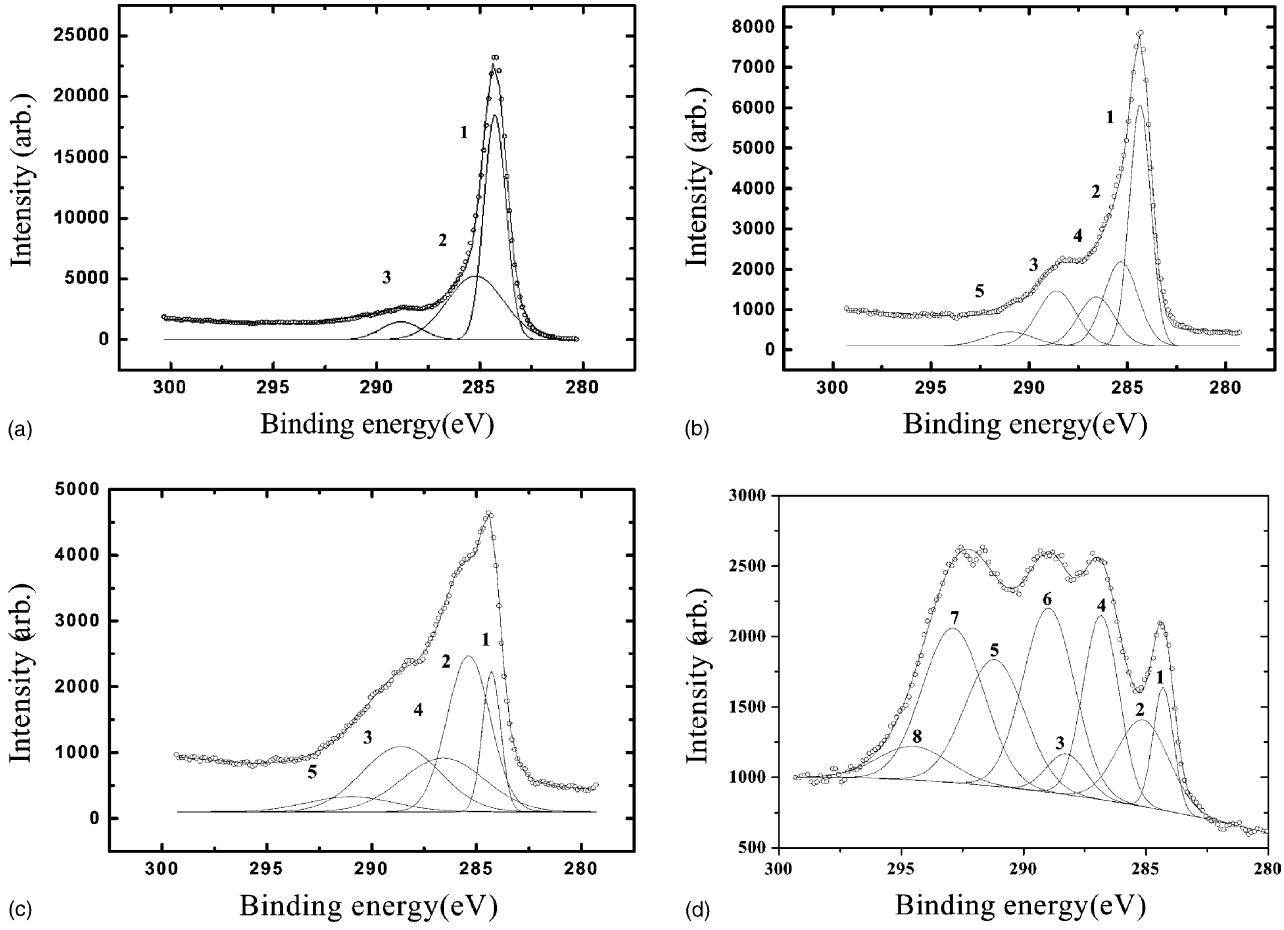

Fig. 1. XPS C 1s curve of the SWCNTS: (a) the undoped; fluorinated at (b) 150, (c) 200 and (d) 300 °C.

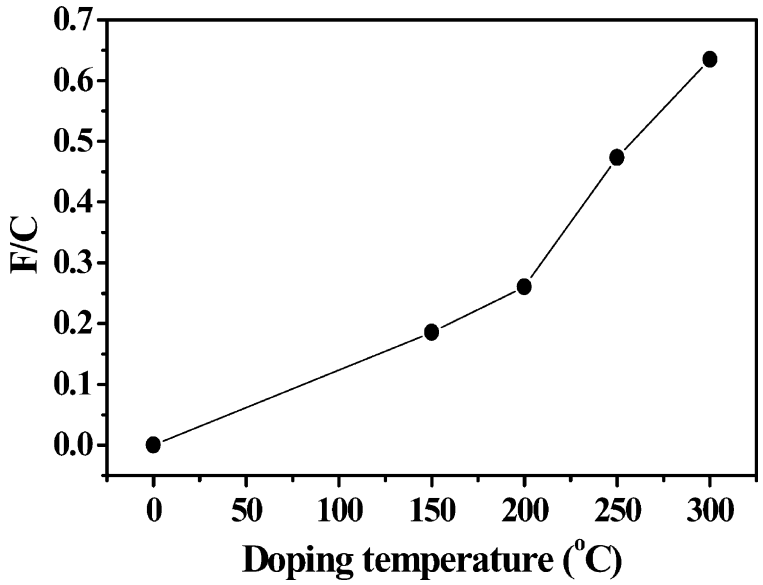

Fig. 3. The surface compositions (F/C) determined by XPS spectra as a function of fluorination temperature.

shape. The intensity of F 1s peak increases and the binding energy shifts toward higher binding energy with reaction temperatures. Nevertheless the binding energy remains within 688 eV at a temperature of up to 200 °C, whereas the binding energy jumps to near 691 eV at the temperature of 250 °C. The latter peak is similar to that of tetrafluoroethylene, which has a strong covalent bonding. The significant shift in the binding energy for the sample fluorinated at higher temperatures indicates that the bonding nature of the samples fluorinated at low temperatures <200 °C is very different from the simple covalent bonding character. This will form a partial ionic bonding in addition to the strong covalent bonds. With increasing temperature, the C 1s and F 1s peaks assigned to fluorine functional groups shift to higher binding energy and their intensities become stronger [9,10].

Consequently, the amount of doped fluorine increases with increasing doping temperature, and the fluorine atoms might be covalently attached to the sidewall of the SWCNTs. If some part of SWCNTs is destroyed by fluorination at high temperature, the inside of nanotubes might be able to be fluorinated. But that could not be confirmed because it is not easy to confirm whether or not fluorine is doped on inside of them. At low temperatures of up to 200 °C, they show an ionic bonding character (semi-ionic) which implies the sidewall functionalization, whereas at high temperatures the binding energy shifts to higher binding side, revealing a covalent bonding character of $(CF)_n$, which implies resistivity increase by enhancing sp^3 bonding and disintegration of nanotube walls, as can be confirmed later by the four-point resistivity.

The surface compositions (F/C) determined by the peak area of C 1s and F 1s XPS spectra are shown in Fig. 3. The value increases with the increasing temperature and reaches close to 0.5 at 250 °C, in good agreements with the previous reports, although the fluorination condition is different from our experiment [5,8]. At 300 °C, this value reaches 0.65. Since CF_x composition with $x > 0.5$ is prohibited in the sidewall fluorination due to electrostatic repulsion between fluorine atoms, we can only imagine this in terms of a new phase formation. This is in good agreement with IR results as shown in Fig. 4. Infrared spectroscopy (KBr pellet method) confirmed the presence of semi-ionically and covalently bonded fluorine atoms in the same F–SWCNTs. As we can see this Fig. 4, a band at 1100 cm^{-1} assigned to the semi-ionic C–F bonds decreases and a band at 1210–1250 cm^{-1}, a characteristic of the C–F covalent bonds, increases with reaction temperatures. There are also typical bands that indicated due to a very small amount of moisture (OH) and CO_2 in air at about 3400 and 2350 cm^{-1}, respectively.

Fig. 5(a) shows a TEM image of untreated SWCNTs. Fig. 5(b) shows the TEM image of SWCNTs fluorinated at 150 °C. The untreated SWCNT bundles with a diameter of 1.5 nm are clearly shown in Fig. 5(a), which is in good agreement with the value estimated from the Raman breathing mode (see Fig. 7). As can be also seen from Fig. 5(b), the tubes remain largely intact after fluorination at 150 °C.

Fig. 6(a)–(d) show the TEM image of SWCNTs fluorinated at 300 °C. These bundles are transformed into multi-wall-like phase after fluorination at 300 °C under our fluorination condition, as shown in Fig. 5(a). Mickelson et al. have also reported that the SWCNTs fluorinated at 500 °C are essentially all destroyed, and some MWCNT-like structures are generated [4].

As can be seen from these images Fig. 7(a)–(d), it was also thought that nanotube phase changed during the TEM observation of F-SWCNTs. The phase transformation such as MWCNTs-like (Fig. 6(a)), onion (Fig. 6(b) and graphitic structure (Fig. 6(c)) takes place owing to the electron beam-induced, which was never observed from the undoped

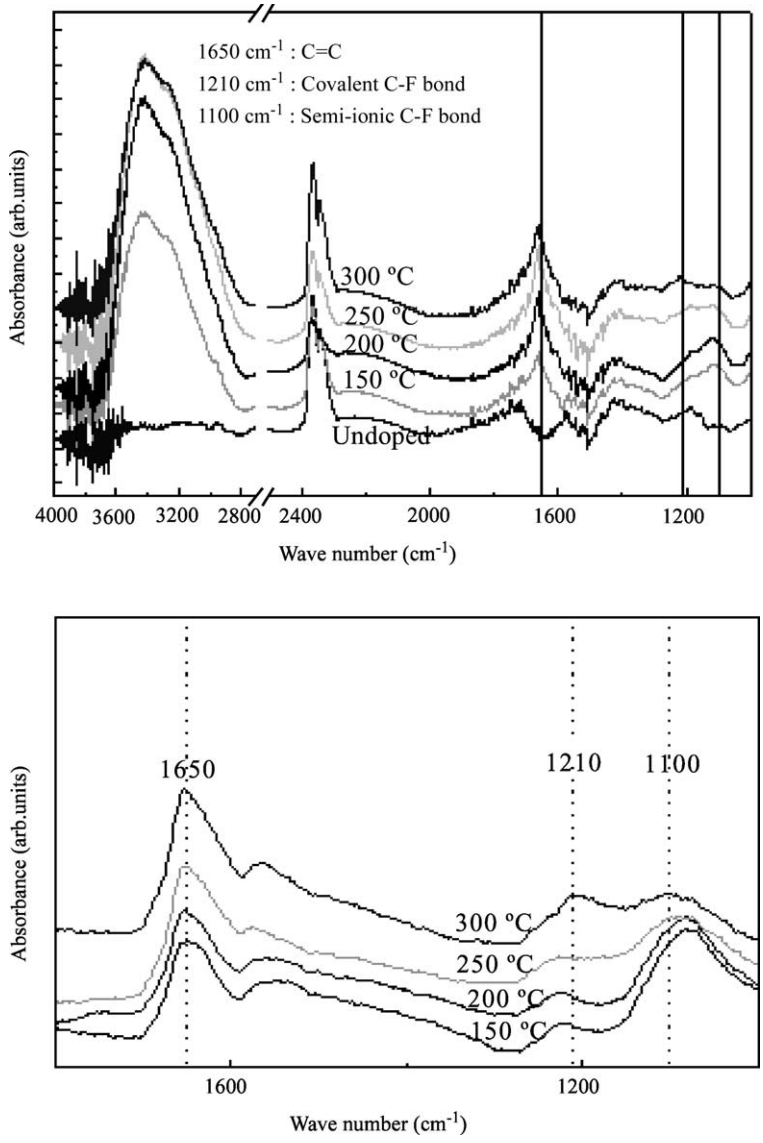

Fig. 4. FT-IR data of the SWCNTs fluorinated at various fluorination temperatures.

nanotubes. Besides the graphitic-layered phases, we also observed an amorphous and turbostratic phases (Fig. 6(d)) [11].

As can be known from Figs. 5 and 6, the structural transformation strongly depends on the reaction temperature, i.e. the doping content. One important practical aspect of the fluorinated CNTs is the significant enhancement of the wettability in water. The fluorinated CNTs were completely dispersed without aggregation for several months, unlike the pristine CNTs in water, where the CNTs easily aggregate. This property may be important in energy storage particularly in improving the capacitance in the supercapacitor and nanocomposites with various organic solutions as well.

The Raman spectra of undoped and SWCNTs fluorinated at various temperatures are shown in Fig. 7. The smaller peak near 200 cm^{-1} of undoped and SWCNTs fluorinated at 150 °C is due to a characteristic-breathing mode of the SWCNTs. This breathing mode is suppressed by F-doping up to 150 °C. Each spectrum also consists of a distinctive pair of broadband at 1580 (G band) and 1360 cm^{-1} (D band). The Raman peaks correspond to sp^2 and sp^3 carbon stretching modes, respectively. The I_G/I_D peak intensity ratios decease with increasing fluorination temperature, indicating change in their structural properties in the bulk after fluorination.

From these Raman spectra and HRTEM study, the strong of fluorination of the SWCNTs leads to the breaking of carbon–carbon bonds and the disintegration of tube structure. Structural transformation of fluorinated SWCNTs may be also induced by electron-beam irradiation during the transmission electron microscope observation.

Fig. 8 also shows the resistivity of the F-SWCNTs mat measured by the four-point probe method at room temperature. It can be seen that the resistivity increases with

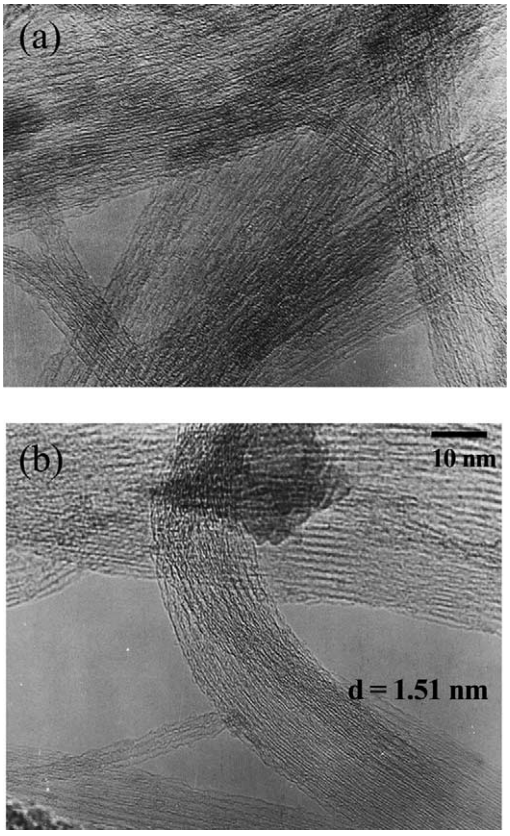

Fig. 5. High-resolution TEM image of the SWCNTs: (a) the undoped; fluorinated at (b) 150 °C.

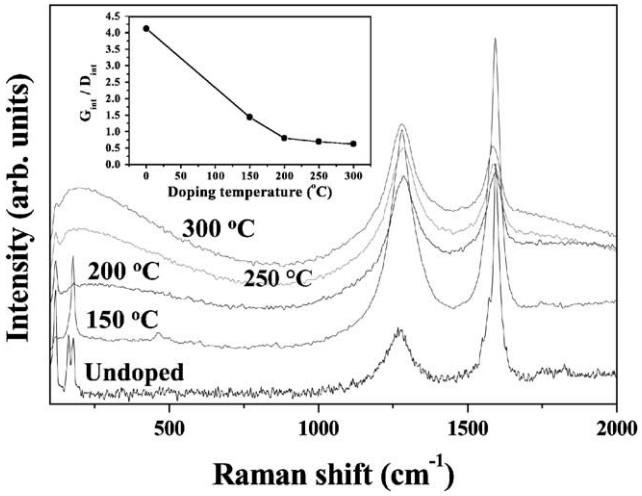

Fig. 7. FT-Raman spectra of the SWCNTs fluorinated at various fluorination temperatures.

increasing reaction temperatures, i.e. the F-doping content corresponding to the similar trend of the XPS data. The electronic properties are altered by fluorination so as to decrease the conductivity of the individual SWCNTs.

3. Experimental details

Single-walled carbon nanotubes (SWCNTs) were prepared by the conventional catalytic arc discharge. The stainless

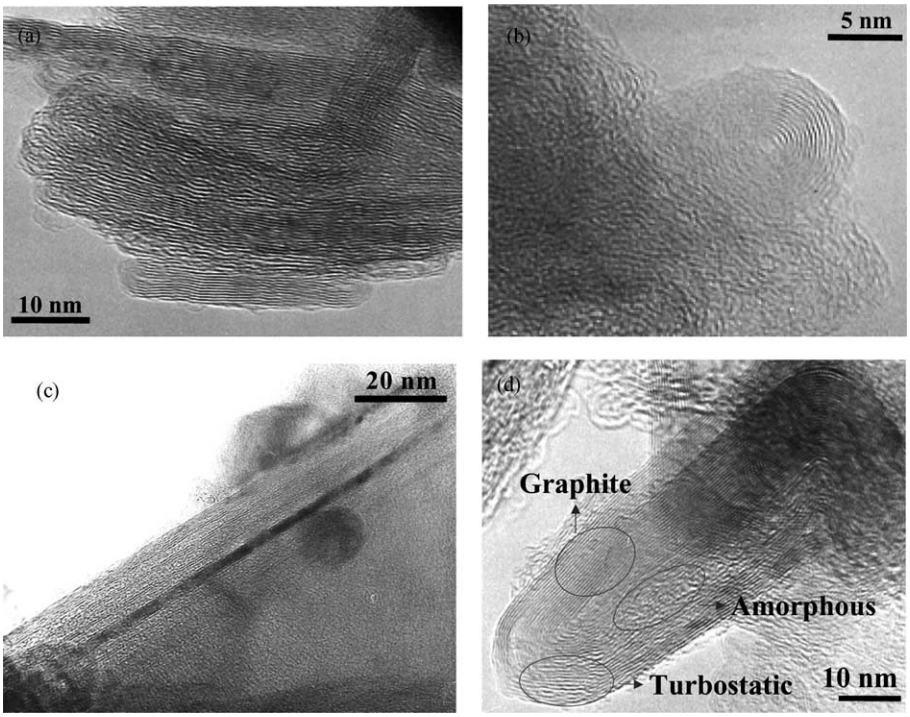

Fig. 6. High-resolution TEM image of the SWCNTs fluorinated at 300 °C.

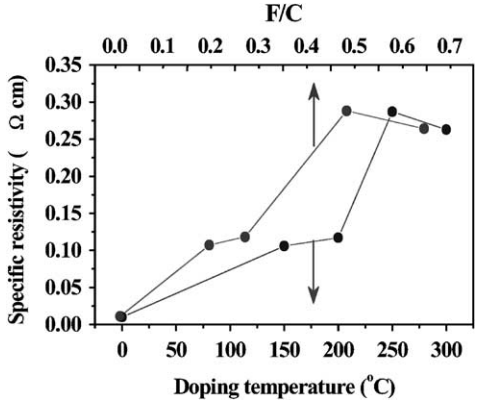

Fig. 8. The resistivity measured by the four-point probe method from the pelletized fluorinated samples at room temperature.

chamber was 150 mm in diameter and the reactor is 150 mm in length. The chamber was pumped out to a base pressure of 100 mtorr and then helium was introduced until the pressure reaches to 100 torr. The voltage between two graphite rods was fixed to be 25 V. By moving the anode forward, arc discharge is started and kept for 5 min till the anode was completely consumed. The current was maintained in the range of 60–80 A. The total amounts of catalysts in a graphite powder were fixed at 5 wt.%, with the ratio of the transition metals (Ni:Co:FeS = 1:1:1). The powder was collected from the chamber, collar, and cathode and then grinded together. This powder was used for fluorination without purification. The purity of single-walled carbon nanotubes in this powder is about 30%. The detail has been described elsewhere [12]. This powder was brought into a Ni boat of the fluorine reaction chamber made by Ni and SUS-316 in order to prevent erosion.

Single-walled carbon nanotubes (SWCNTs) were fluorinated at several different temperatures. The reaction was performed following process described in detail elsewhere [12,13] known to be efficient for the fluorination of carbon fibers. SWCNTs were introduced in a nickel reactor having a Teflon gasket. Prior to fluorination, the chamber was pumped out to a basal pressure of 10 mtorr and purged by nitrogen gases to remove the residual oxygen gases and moisture. Fluorine gas was then introduced and the pressure of 20 KPa was maintained for 10 min for a given reaction temperature. After the reaction, the chamber was pumped out again to 10 mtorr and nitrogen gas was refilled prior to the extraction of the powder sample [14].

The four-point method was used for the measurement of resistance of a single walled carbon nanotubes. F-SWCNTs mat was prepared by 1000 psi of pressure without any binder to measure the resistance of SWCNTs. The prepared mat is pellet type with about 15 mm of diameter and 1 mm of thickness. F-SWCNTs mat was cemented with silver paint to Pt leads, printed on an alumina plate. This avoids the problems caused by contact resistance. The constant current passing through the fiber was 20 μA. The specific resistance is calculated taking into account the diameter and the length of specimen. Measurements were done on several F-SWCNTs of the same sample. The specific resistance of a F-SWCNTs (ρ) was calculated using the mat length l ($l = 1$ mm) and its diameter d ($d = 15$ mm) using the following equation.

$$\rho = R\pi\frac{(d/2)2}{l} = \frac{R\pi d^2}{4l} = \frac{1}{\kappa} \quad (1)$$

where κ is the specific conductivity.

The fluorinated SWCNTs were characterized by measurement of resistivity, Fourier transformed (FT) Raman spectroscopy, XPS and the observation of TEM (200 kV FE-gun, Jeol, JEM-3011). The resistivity was measured by four-point probe method after pelletizing the powder. The structure was analyzed by Fourier transformed (FT) Raman spectroscopy (BRUKER, RFS 100/S), and X-ray photoelectron spectroscopy (XPS, Ulvac Phi Model 5500, Mg Kα radiation).

References

[1] S. Iijima, T. Ichihashi, Nature (London) 363 (1993) 603–605.
[2] A. Hamwi, H. Alvergnat, S. Bonnamy, F. Beguin, Carbon 35 (1997) 723–728.
[3] A.C. Dillon, K.M. Jones, T.A. Bekkedahl, C.H. Kiang, D.S. Bethune, M.J. Heben, Nature (London) 386 (1997) 377–379.
[4] E.T. Mickelson, C.B. Huffman, A.G. Rinzler, R.E. Smalley, R.H. Hauge, J.L. Margrave, Chem. Phys. Lett. 296 (1998) 188–194.
[5] E.T. Mickelson, I.W. Chiang, J.L. Zimmerman, P.J. Boul, J. Lozano, J. Liu, R.E. Smalley, R.H. Hauge, J.L. Margrave, J. Phys. Chem. B 103 (1999) 4318–4322.
[6] K.F. Kelly, I.W. Chiang, E.T. Mickelson, R.H. Hauge, J.L. Margrave, X. Wang, G.E. Scuseria, C. Radolff, N.J. Halas, J. Phys. Chem. B103 (1999) 440–445.
[7] T. Nakajima, S. Kasanatsu, Y. Matsuno, Eur. J. Solid Inorg. Chem. 33 (1996) 831–840.
[8] H. Touhara, F. Okino, Carbon 38 (2000) 241–267.
[9] H. Touhara, J. Inahara, T. Mizuno, Y. Yokoyama, S. Okanao, K. Yanagiuch, I. Mukopadhyay, S. Kawasaki, F. Okino, H. Shirai, W. Xu, T. Kyotani, A. Tomita, J. Fluorine Chem., in press.
[10] K.H. An, J.G. Heo, K.G. Jeon, D.J. Bae, C. Jo, C.W. Yang, C.Y. Park, Y.H. Lee, Y.S. Lee, Y.S. Chung, Appl. Phys. Lett. 80 (2002) 4235–4237.
[11] J.C. Bokoros, in: P.L. Walker Jr., (Ed.), Chemistry and Physics of Carbon, vol. 5, Marcel Dekker, New York, 1969, Chapter 1, pp. 7–23.
[12] Y.S. Park, K.S. Kim, H.J. Jeong, W.S. Kim, J.M. Moon, K.H. An, D.J. Bae, G.S. Park, Y.S. Lee, Y.H. Lee, Synth. Metals 126 (2002) 245–251.
[13] A. Bismarck, R. Tahhan, J. Springer, A. Schulz, T.M. Klapötke, H. Zell, W. Michaeli, J. Fluorine Chem. 84 (1997) 127–134.
[14] Y.S. Lee, B.K. Lee, Carbon 40 (2002) 2461–2468.